Spin–orbit splitting in graphene on metallic substrates

2011 J. Phys.: Condens. Matter 23 225502

(http://iopscience.iop.org/0953-8984/23/22/225502)

J. Phys.: Condens. Matter **23** (2011) 225502 (6pp) doi:10.1088/0953-8984/23/22/225502

Spin–orbit splitting in graphene on metallic substrates

Z Y Li[1,2], Z Q Yang[1,3], S Qiao[1], J Hu[4] and R Q Wu[4]

[1] State Key Laboratory of Surface Physics and Department of Physics, Fudan University, Shanghai 200433, People's Republic of China
[2] College of Science, University of Shanghai for Science and Technology, Shanghai 200093, People's Republic of China
[3] Department of Chemistry, Northwestern University, Evanston, IL 60208, USA
[4] Department of Physics and Astronomy, University of California, Irvine, CA 92697-4575, USA

E-mail: zyang@fudan.edu.cn

Received 28 March 2011, in final form 18 April 2011
Published 17 May 2011
Online at stacks.iop.org/JPhysCM/23/225502

Abstract
Substrate-induced spin–orbit splitting in graphene on Ni, Au and Ag(111) is examined on the basis of density-functional theory. The Rashba splitting of π bands along the ΓM direction of the graphene surface Brillouin zone in graphene on Ni(111) is found to be very small (a few millielectronvolts), consistent with the experimental report of Rader *et al*. Instead, very strong Rashba splitting (near 100 meV) can be obtained for graphene with a certain stretch distortion on a Au substrate. It can be ascribed to the effective match in energy between the C 2p and Au 5d bands, obtained from the analysis of densities of states. The net charge transfer between the graphene and the substrates just affects the spin–orbit effect indirectly. The small spin–orbit splitting induced by the Ag substrates indicates that heavy metals do not always produce large SO splitting. Our findings provide important insights that are useful for understanding the metal-induced Rashba effect in graphene.

(Some figures in this article are in colour only in the electronic version)

1. Introduction

Graphene has attracted extensive attention in recent years due to its unique and remarkable electronic properties, such as the gapless-semiconductor band structure, the existence of pseudospin, and the high electronic mobility at room temperature [1–3]. These features are highly desirable for the development of the next-generation microelectronic and spintronic devices [4, 5]. It was found that spin currents in graphene can be manipulated using various electronic tactics, in particular through spin–orbit (SO) interactions, which are now among the most active research topics in several realms [6, 7]. No magnetic materials or fields are needed during such processes [6, 7]. The intrinsic SO effect in pure graphene layers is nevertheless very weak, 0.1–0.37 meV [8–10] or even smaller [11], in flat graphene sheets or carbon nanotubes due to the low nuclear charge of the carbon atom. This SO effect in pure graphene is too small to be used practically.

It was very exciting when Dedkov *et al* reported an extraordinarily large Rashba [12] SO splitting (225 meV) for the π states along ΓM of epitaxial graphene on a Ni(111) substrate through their angle-resolved photoemission studies [13]. However, this result was challenged by Rader *et al* [14] who found that the sum of Rashba and exchange splitting in the graphene layer on either Ni(111) or Co(0001) is less than 45 meV. They further argued that the Rashba effect in graphene may only be enhanced by adding some heavy metals, such as Au, to the system [14]. Though some theoretical studies of the SO effect in graphene have been reported [11, 15, 16], the contradictory experimental results for the SO splitting in graphene [13, 14] have not been clarified up to the present. In addition, there have also been no systematical studies of how the metallic substrates affect the SO splitting in graphene and what the mechanism of substrate-induced SO splitting in graphene is. Clearly, the solutions to these problems are crucial for the progress of graphene physics.

In this paper, we report results of density-functional theory (DFT) [17] calculations for the electronic and spin-polarized properties of graphene on Ni, Au and Ag(111) substrates. The Ni substrate is found to not produce large SO

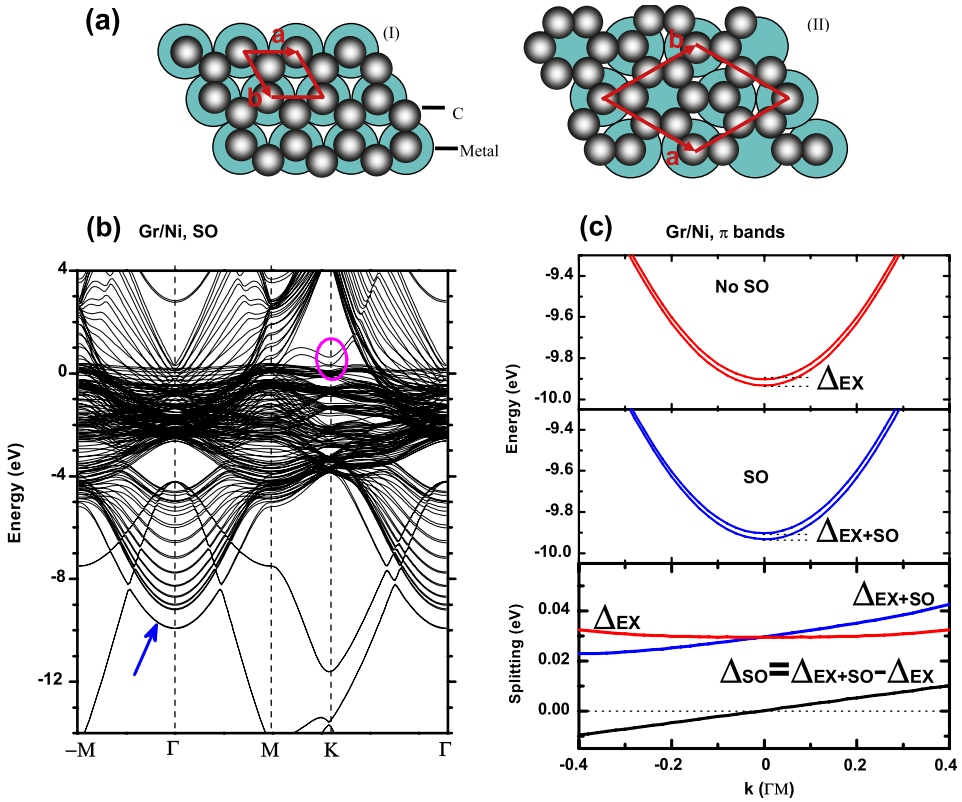

Figure 1. (a) Two possible configurations of graphene adsorbed on metal (111) substrates. The rhombus gives the unit cell with vectors **a** and **b** along the graphene plane. (b) The energy bands of Gr/Ni in configuration (I) with SO interaction. The blue arrow indicates the graphene π bands around Γ. The magenta oval shows the position of the Dirac point. (c) The enlarged π bands around Γ without or with SO interaction. The exchange and/or SO splitting of the bands is also given. The k point in (c) is in the unit of the vector ΓM.

splitting in graphene, consistent with the experimental results of Rader *et al* [14]. The reason is ascribed to the sizable energy mismatch between the C 2p bands and Ni 3d bands. Interestingly, the SO splitting of graphene on Au substrates can be significantly enhanced due to strong hybridization of the graphene p_z state and the metal d_{z^2} state, especially for a system with a large lateral stretch in the graphene lattices. The net charge transfer between graphene and the substrates just affects the spin–orbit effect indirectly, not supporting the effective electric field model proposed in [13] to explain the SO effect in graphene. The small SO splitting induced by Ag substrates indicates that heavy metals do not always generate large SO splitting. Very few atomic layers of metal substrates are sufficient to produce large SO splitting.

2. Models and analysis

The electronic structures of graphene on metal (111) substrates, abbreviated as Gr/M (M = Ni or Au), were calculated by using the Vienna *ab initio* simulation package (VASP) at the level of the local-spin-density approximation (LSDA) [18][5]. Projector-augmented wave (PAW) pseudopotentials were employed to describe the effect of the ionic cores. The Gr/M systems were modeled by a periodic slab geometry, with a vacuum of at least 10 Å between two neighboring slabs. Face center cubic structures were adopted for all the metal substrates considered. Each slab contains one graphene layer and N metal layers. The equilibrium structures were optimized until the Hellmann–Feynman forces became less than 0.05 eV $Å^{-1}$ [19]. The energy cutoff in the calculations was set to be 400 eV, and the total energy was converged to better than 10^{-5} eV. The SO coupling term considered takes the form of $H_{SO} = \frac{\hbar}{4m^2c^2}\frac{1}{r}\frac{\partial V_{eff}}{\partial r}(\mathbf{r}\times\mathbf{P})\cdot\sigma$, where V_{eff} is the effective potential of the electrons, $\mathbf{P}$ is the momentum operator, and $\sigma \equiv (\sigma_x, \sigma_y, \sigma_z)$ are the Pauli matrices. In two-dimensional electron gases (2DEGs), due to the structure inversion asymmetry, the SO coupling term can be simplified to the Rashba SO interaction, $H_R = \alpha_R(P_x\sigma_y - P_y\sigma_x)$, where the Rashba strength α_R depends on the gradient of the potential along the direction perpendicular to the 2DEG plane [12]. A sizable Rashba effect has been detected in several metallic surfaces by spin- and angle-resolved photoemission, such as Au(111), Ag(111), and Bi/Ag(111) [20–22]. Two Gr/M adsorption configurations [23–25] were considered, as depicted in figure 1(a). We found that configuration (I) is more stable for graphene on Ni(111), as it gives a very small lattice mismatch (∼1%). For the same reason, configuration (II) is preferred for graphene on the larger Au(111) lattices [24]. k-point grids of 31×31 and 11×11 were employed to sample the Brillouin zones of configurations (I) and (II), respectively. As

[5] The LSDA is found to describe well the correlation effects of the systems. For example, the distribution of Ni 3d obtained is in good agreement with the results from experimental photoemission spectroscopy [27].

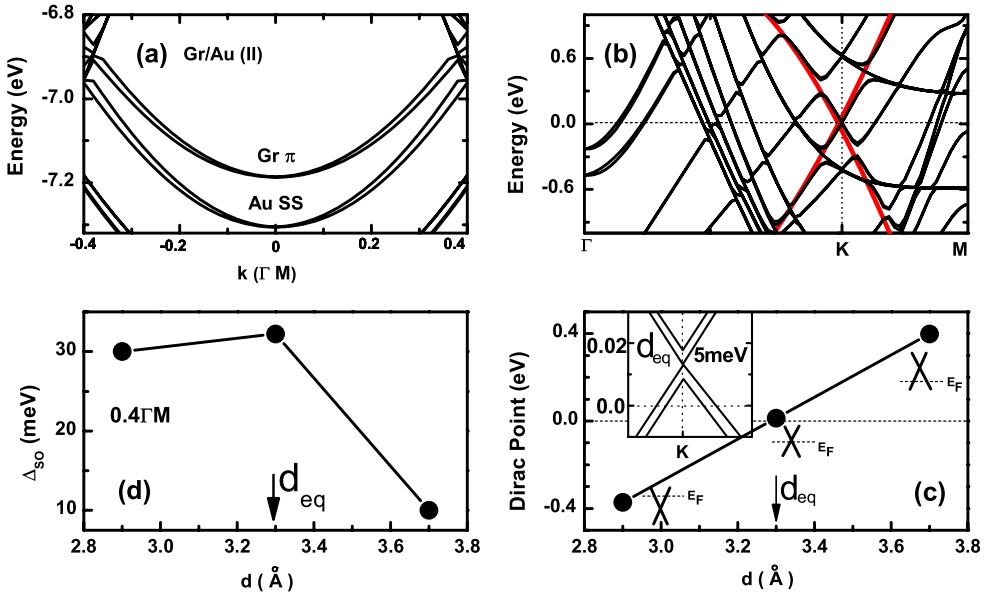

Figure 2. The bands of Gr/Au in configuration (II) with $d_{eq} = 3.3$ Å: (a) around -7.0 eV along $-M\Gamma M$ and (b) near E_F along $\Gamma K M$. The red lines in (b) are drawn to indicate the Dirac point. Parts (c) and (d) give the position of the Dirac point and the SO splitting of the π bands at 0.4 ΓM versus the distance between the graphene and the substrate, respectively. The inset in (c) shows the enlarged bands near the Dirac point of (b), where the SO splitting is about 5 meV. The rough position of the Dirac point relative to E_F is also given in (c) for each case.

a benchmark calculation for the SO effect, we first determined the SO splitting of the surface state (SS) near the Fermi level (E_F, set as energy zero) of the pure Au(111) film [22]. Our result, $\Delta E_{SO} \sim 100$ meV, agrees well with the data in [22].

3. Results and discussion

The band structures of Gr/Ni with the number of metal layers $N = 13$ [25] are given in figures 1(b) and (c). We have checked that more Ni atomic layers do not improve the results. The distance between the graphene and Ni(111) film is optimized to be 2.0 Å. The direction of Ni magnetization is set to be in-plane and perpendicular to the ΓM axis. In figure 1(b), the comparatively flat and less-dispersing bands below E_F are mainly composed of Ni 3d states. Three Ni SSs are hiding in the dense bands from 0.0 to -2.5 eV and can be observed clearly by enlarging the figures. The multiple parabolic bands appearing between -4 and -9 eV are mainly the bands from the Ni film [26]. Despite the strong perturbation from the Ni(111) substrate, one can still easily trace several graphene bands in figure 1(b), e.g., the graphene σ and π states at -4.0 and -10.0 eV in the vicinity of the Γ point. Compared to the band structures of pure graphene, these states are now spin polarized, and shifted downward in energy by about 1.2 and 2.2 eV, respectively. In particular, the features of conical points at the K-point near E_F, in the region highlighted by a magenta oval in figure 1(b), are destroyed due to the broken equivalence of the A and B sublattices. These results are in good agreement with photoemission measurements [27]. In configuration (I), A- and B-type carbon atoms are on the atop and hollow sites separately over Ni(111) and hence their on-site energies are modulated differently by the substrate.

Now we zoom in to explore the SO splitting of the π states of graphene along the $-M\Gamma M$ line, following the convention in the literature [13, 14, 28]. To distinguish contributions from different factors, we studied the cases with and without the SO interaction separately. As illustrated in figure 1(c), bands without the SO interaction are symmetric about the Γ point and show an induced exchange splitting (Δ_{EX}) of 30 meV on the magnetic Ni substrate. After inclusion of the SO interaction, the energy splitting (Δ_{EX+SO}) contains two parts: exchange and SO (Δ_{SO}). The Δ_{SO} value can be extracted through $\Delta_{SO} = \Delta_{EX+SO} - \Delta_{EX}$. The linear relationship of Δ_{SO} versus k in figure 1(c) indicates that the SO effect is indeed of Rashba type ($\Delta_{SO} = 2\alpha_R k$, where α_R is the Rashba strength) [12, 14]. The Rashba splitting of the π states of graphene on Ni(111) obtained from our calculations is about 10 meV, consistent with the experimental data in [14]. Although this value is substantially larger than the SO splitting (0.37 meV) in curved graphene [9], it is certainly not as large as that reported by Dedkov *et al* for Gr/Ni(111) [13].

Let us see if Au can further substantially enhance the SO splitting. Au is chemically 'inert' (with completely filled d states) and the equilibrium interlayer distance between the graphene and the Au substrate is $d_{eq} = 3.3$ Å in configuration (II). As given in figures 2(a) and (b), the π bands of the graphene are now around -7.1 eV (relative to E_F) and exhibit more pronounced SO splitting. We want to point out that the Au SS at -7.3 eV [26] in figure 2(a) is actually localized in the opposite side of the Au slab and thus has no interaction with graphene states. The corresponding Au SS in the graphene side moves down and mingles with other Au states when the separation between the graphene and the Au substrate (denoted as d below) is decreased. This can be ascribed to the interactions with the graphene π states. In the equilibrium geometry, the SO splitting of the graphene π bands at 0.4 ΓM is near to 30 meV (cf. figure 2(a)), which is three times larger than that in graphene on the Ni(111) substrate. For

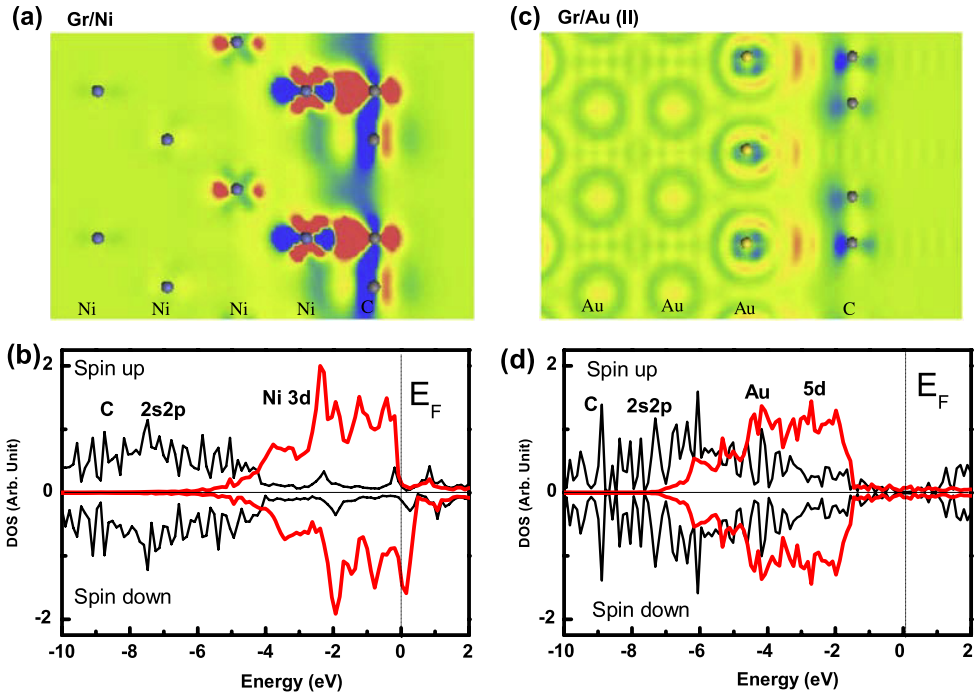

Figure 3. (a) The difference of the charge density between Gr/Ni and isolated graphene plus Ni. The red color indicates gaining electrons, while the blue indicates losing them. (b) The partial densities of states of carbon (2s and 2p) and the first layer Ni atoms (3d) in the Gr/Ni system. Average values were employed due to multiple atoms in the unit cell for each layer. Parts (c) and (d) are the same as (a) and (b), respectively, expect that they are for the Gr/Au(II) system. The contour of the charge density is plotted in the plane perpendicular to the interface; the cut line is along the vector $\mathbf{a} + \mathbf{b}$ in figure 1(a). Note that the values of the C DOSs in (b) and (d) are magnified five times.

Gr/Au in configuration (II), the *A* and *B* sublattices experience the same environment again. As a result, the graphene layer restores its unique electronic feature: the Dirac cone near E_F as highlighted by the red lines in figure 2(b). It is interesting to note that the Dirac point lies right at E_F, a sign which indicates almost no charge transfer between the graphene and the Au in the equilibrium geometry. However, the charge transfer, and therefore the energy position of the Dirac cone, are adjustable through changing the distance between the graphene and the substrate [24]. This is clearly manifested in figure 2(c), where the Dirac point moves down when the separation shrinks from equilibrium, and vise versa. Strikingly, the SO splitting of graphene decreases both ways in figure 2(d) (the same trend is also obtained in Gr/Au(I)), regardless of the direction of charge transfer and strength of the effective electric field at the interface. This finding does not support the effective electric field model proposed in [13, 14] for the explanation of the enhanced SO effect in these systems. The trend is consistent with the conclusion obtained from analytical estimates and Monte Carlo simulations for graphene on SiO_2 substrates [16]. Further important evidence of the interaction between graphene and the substrate is the SO splitting of the Dirac states. Since the intrinsic SO interaction in pure graphene was predicted to be almost zero at this point [29], this splitting is merely induced by the metal substrate. The inset in figure 2(c) shows the calculated SO splitting at the Dirac point: both electron and hole bands show $\Delta_{SO} = 5$ meV, close to the value (13 meV) given in the recent experiment [30].

Since the Rashba splitting in Gr/Ni and Gr/Au(II) is very different, it is meaningful to find the reasons behind it. Figure 3(a) shows the charge density differences ($\Delta\rho$) of Gr/M (defined as $\Delta\rho = \rho_{Gr/M} - \rho_M - \rho_{Gr}$). Substantial charge redistribution occurs at the interface between graphene and Ni. The graphene p_x and p_y states and the Ni d_{z^2} state lose electrons while graphene p_z and Ni d_{xy} gain electrons. Bader charge analysis indicates that each carbon atom on top of Ni gains 0.15 electrons and the one on the hollow site gains 0.02 electrons. Meanwhile, each Ni atom right under a carbon atom loses 0.19 electrons, to graphene and also to other atoms. The charge redistribution causes a large downward shift of the graphene bands. For example, the π bands move from -7.8 eV (at the Γ point) in pure graphene to -10.0 eV in Gr/Ni (figure 1(b)). With consideration of the work functions of the two systems (4.7 eV (Gr) and 3.8 eV (Gr/Ni)), the net downward shift of the π bands at the Γ point of graphene in Gr/Ni is 1.3 eV, compared to that in pure graphene. Meanwhile, the Ni d bands are pinned against the E_F. As a result, the C p_z and the Ni d_{z^2} states have a large energy mismatch and thereby hybridize very weakly. The band mismatch in Gr/Ni can be seen more obviously in the partial densities of states (DOSs) of carbon and the first layer Ni atoms (figure 3(b)). The Ni 3d states are mostly above -4 eV, while the C 2p states are well below them. Thus, the energy mismatch of C 2p and Ni 3d bands determines the small SO strength in the Gr/Ni system.

For the Gr/Au(II), the charge redistribution is given in figure 3(c). Bader charge analysis shows that charge gain and loss between the atoms in Gr/Au(II) is negligible ($<0.002e$), consistent with the small shift of the Dirac point in the inset of figure 2(c). In spite of the negligible net

Table 1. The wavefunction components of the graphene π bands at Γ for the considered systems at equilibrium distances. The values are in the scale of the graphene p_z state. The bold type expresses the more stable configuration. The SO splitting (in millielectronvolts) of the graphene π bands in configuration (I) was given at $k = 0.25\ \Gamma M$, while in configuration (II) it was at $k = 0.5\ \Gamma M$ due to the double lattice vectors. N expresses the number of metal layers adopted.

	Ni(**I**) ($N = 13$)	Au(**II**) ($N = 9$)	Au(I) ($N = 12$)	Ag(**II**) ($N = 9$)	Ag(I) ($N = 12$)
Gr-p_z state	1.0	1.0	1.0	1.0	1.0
M-s state	0.8	1.3	0.1	0.5	0.7
M-d_{z^2} state	0.0	2.4	1.3	0.0	3.7
SO splitting	6.3	32.2	89.0	1.6	36.9

charge transfer between graphene and Au, charge redistribution occurs, especially extending into the Au substrate. At the interface, the C p_z and Au $d_{xz,yz}$ states tend to lose electrons to the s bands. Compared to pure graphene, the π bands at the Γ point in Gr/Au(II) shift upward by 0.6 eV, opposite to the trend in Gr/Ni. Meanwhile, the locations of the Au 5d bands are in a lower energy region: the bottoms of the Au d bands extend to below -7 eV (see figure 3(d)). These two behaviors give rise to a nice match in energy between the C 2p and the Au 5d states, leading to the large SO splitting in graphene in the system. Thus, the 'inert' metal is a benefit for the production of large SO splitting in the graphene π bands. Since charge transfer between graphene and the metal substrates may affect the band match between the C 2p and the metal d, it may vary the SO strength in the graphene bands indirectly.

To further appreciate the different band intermixings in the Gr/Ni and Gr/Au cases, we quantitatively analyzed the wavefunction compositions of the graphene π bands at Γ. As shown in table 1, the mixing ratio of C $2p_z$:Ni 4s in Gr/Ni(I) is about 1.0:0.8; no Ni 3d is involved. Due to the mixing of the C $2p_z$ and Ni 4s states in the interface, the potential symmetry at the two sides of graphene is broken and a Rashba splitting (6.3 meV) is induced in the Gr/Ni system. The Ni 4s states, however, do not generate a large SO effect in the graphene π bands due to the small $\frac{1}{r}\frac{\partial V}{\partial r}$ of s electrons, from an atomic point of view. In contrast, the Au d_{z^2} state is obviously responsible for the large SO splitting in the graphene π bands in Gr/Au(II); the ratio of C $2p_z$:Au 6s:Au 5d is about 1.0:1.3:2.4. Thus, appropriate intermixing of the d_{z^2}-like metal surface states with the graphene p_z state is a key factor for producing large SO splitting in graphene. It was discussed that pure p or d states cannot produce strong Rashba splitting [31]. Actually, the hybridization between p or d states in Gr/Au(II) not only allows the large SO effect of Au to penetrate into graphene, but also introduces and enhances the asymmetry around graphene since the 'bonding' orbits have their weights only below the graphene layer. Therefore, local SO coupling, hybridization, and potential asymmetry are interconnected for the enhancement of the Rashba splitting in the systems. For certain metal substrates, the SO strength of the graphene π bands may vary greatly due to the different band-matching strengths between the graphene and the metal substrates.

For spintronic applications, it is desired to make the SO effect large and controllable [8–10]. Although configuration (I)

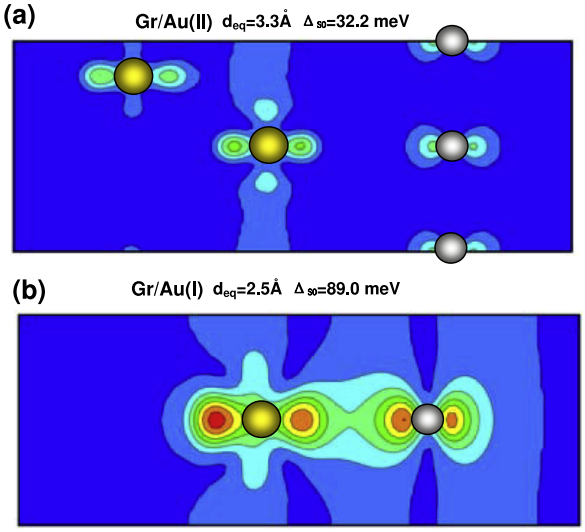

Figure 4. (a) The charge density at the Γ point in the graphene π bands in the Gr/Au(II) system with equilibrium distance between the graphene and the Au substrate. (b) The corresponding charge density in Gr/Au(I). The density is plotted in the plane perpendicular to the interface; the cut line is along the vector **a** in figure 1(a). More effective hybridization between C $2p_z$ and Au $5d_{z^2}$ is formed in Gr/Au(I).

depicted in figure 1 is unstable for Gr/Au, due to the need for a large stretch for the C–C bonds (by 17%), the reduced interlayer distance (2.5 Å) and the subsequently enhanced spatial overlap between the graphene and Au orbitals allows us to further explore the SO effects for different contact models. The graphene π bands in Gr/Au(I) disperse less and shift upward as well because of the expansion of the C–C bond length. This makes a better match between the C p bands and the metal d bands compared to Gr/Au(II). As given in table 1, the ratio of C $2p_z$:Au 6s:Au 5d is about 1.0:0.1:1.3. Obviously, the hybridization between the C $2p_z$ and Au 5d states in Gr/Au(I) is more effective than that in Gr/Au(II). Indeed, the single-state charge densities of the graphene π state at the Γ point in figure 4 show that it becomes a mixture of C and Au states in both Gr/Au(I) and Gr/Au(II). Nevertheless, both the strength of hybridization and the induced asymmetry in Gr/Au(I) are obviously much stronger. Therefore, lattice expansion is possibly an effective means to enhance the SO effect in graphene.

Table 1 also contains the results of Gr/Ag(I) and (II). Similarly, the SO splitting in configuration (II) is much less than that in (I) due to the mismatch of the C 2p and Ag 4d bands. While the graphene p_z state has a strong interaction with the Ag d_{z^2} state in configuration (I), only the Ag s state is involved in the more stable Gr/Ag(II), similarly to Ni. As shown in table 1, the smaller SO splitting in Gr/Ag(II) induced by the Ag substrates than that by the Ni substrates indicates that heavier metals do not always produce larger SO splitting. Further, the nuclear charge of Ag ($Z = 47$) is much larger than that of Ni ($Z = 28$). The SO splitting in the Ag(II) case is, however, smaller than that in the Ni(I) case (table 1). Thus, heavier metals may not always produce larger SO splitting in the graphene of Gr/M systems, although the role of nuclear charge is usually believed to be very important for producing

Table 2. The SO splitting (in millielectronvolts) of the π bands of graphene on different metal substrates with the number of metal layers $N = 1$ and 6. The value is given at $k = 0.25$ or 0.5 ΓM, as stated in table 1. The bold type indicates the more stable configuration.

meV	Ni(**I**)	Au(**II**)	Au(I)	Ag(**II**)	Ag(I)
$N = 1$	6.7	11.2	35.4	2.6	6.7
$N = 6$	6.3	33.4	88.0	2.4	41.8

large SO splitting. The effective match in energy of the C 2p and metal d bands in Gr/M is also one of the preconditions. This trend is counterintuitive.

Finally, we also explored the effect of the thickness of the metal films. The SO splittings of the graphene π bands for Gr/Au(I) and (II) and Gr/Ag(I) with $N = 6$ in table 2 are almost the same as the values listed in table 1. For the other two cases, Gr/Ni(I) and Gr/Ag(II), just one monolayer of metal substrate is sufficient to give a saturated SO splitting of the graphene. Since the Au SSs usually extend several atomic layers into the bulk [26], a few layers of metal are needed to obtain the saturated SO splitting. Nevertheless, the SO splitting for graphene on Au mono- and bi-layer films is already large, explaining why one Au atomic layer intercalated between graphene and Ni(111) can cause a substantial Rashba effect in the experiment [30].

4. Conclusions

In conclusion, we investigated the factors that determine the SO splitting of graphene bands on Ni, Au and Ag(111) substrates through systematic first-principles calculations. While the Rashba splitting in Gr/Au is sizable, the effect for Ni and Ag in stable geometries is very limited. The energy match/mismatch of the C 2p and metal d bands was identified as a chief factor in determining the SO strength in graphene on metallic substrates. The SO splitting does not sensitively depend on the net charge transfer between the graphene and the substrates, which may affect the SO strength indirectly through the band match/mismatch. Lateral stretch of the graphene bonds can be an effective way to enhance the SO strength. Heavy metals are found not to always induce large SO splitting in graphene. A few atomic layers of metals are sufficient to produce a saturated strong Rashba splitting in graphene due to the localization of the surface states of metals.

Acknowledgments

The work was supported by the National Natural Science Foundation of China under grant No. 10674027, 973-projects under grant Nos 2006CB921300 and 2011CB921803, the China Scholarship Council, Fudan High-end Computing Center, and Chemistry and Materials Research Division (MRSEC program) of the NSF in USA. The work at UCI was supported by DOE grant DE-FG02-05ER46237 and computing time at NERSC.

References

[1] Castro Neto A H, Guinea F, Peres N M R, Novoselov K S and Geim A K 2009 *Rev. Mod. Phys.* **81** 109
[2] Novoselov K S, Geim A K, Morozov S V, Jiang D, Katsnelson M I, Grigorieva I V, Dubonos S V and Firsov A A 2005 *Nature* **438** 197
[3] Zhang Y, Tan Y-W, Stormer H L and Kim P 2005 *Nature* **438** 201
[4] Tombros N, Jozsa C, Popinciuc M, Jonkman H T and Van Wees B J 2007 *Nature* **448** 571
[5] Semenov Y G, Kim K W and Zavada J M 2007 *Appl. Phys. Lett.* **91** 153105
[6] Datta S and Das B 1990 *Appl. Phys. Lett.* **56** 665
[7] Awschalom D D and Flatte M E 2007 *Nature Phys.* **3** 153
[8] Kane C L and Mele E J 2005 *Phys. Rev. Lett.* **95** 226801
[9] Kuemmeth F, Ilani S, Ralph D C and Mceuen P L 2008 *Nature* **452** 448
[10] Yao Y, Ye F, Qi X-L, Zhang S-C and Fang Z 2007 *Phys. Rev.* B **75** 041401(R)
[11] Gmitra M, Konschuh S, Ertler C, Ambrosch-Draxl C and Fabian J 2009 *Phys. Rev.* B **80** 235431
[12] Rashba E I 1960 *Sov. Phys. Solid State* **2** 1109
Bychkov Yu A and Rashba E I 1984 *JETP Lett.* **39** 78
[13] Dedkov Yu S, Fonin M, Rüdiger U and Laubshat C 2008 *Phys. Rev. Lett.* **100** 107602
[14] Rader O, Varykhalov A, Sánchez-Barriga J, Marchenko D, Rybkin A and Shikin A M 2009 *Phys. Rev. Lett.* **102** 057602
[15] Abdelouahed S, Ernst A, Henk J, Maznichenko I V and Mertig I 2010 *Phys. Rev.* B **82** 125424
[16] Ertler C, Konschuh S, Gmitra M and Fabian J 2009 *Phys. Rev.* B **80** 041405(R)
[17] Kresse G and Furthmüller J 1996 *Phys. Rev.* B **54** 11169
Kresse G and Hafner J 1994 *Phys. Rev.* B **49** 14251
[18] Perdew J P and Wang Y 1992 *Phys. Rev.* B **45** 13244
[19] Durgun E, Senger R T, Sevinçli H, Mehrez H and Ciraci S 2006 *Phys. Rev.* B **74** 235413
[20] Meier F, Dil H, Lobo-Checa J, Patthey L and Osterwalder J 2008 *Phys. Rev.* B **77** 165431
[21] Hoesch M, Muntwiler M, Petrov V N, Hengsberger M, Patthey L, Shi M, Falub M, Greber T and Osterwalder J 2004 *Phys. Rev.* B **69** 241401(R)
[22] Nicolay G, Reinert F, Hüfner S and Blaha P 2001 *Phys. Rev.* B **65** 033407
[23] Karpan V M, Giovannetti G, Khomyakov P A, Talanana M, Starikov A A, Zwierzycki M, Van Den Brink J, Brocks G and Kelly P J 2007 *Phys. Rev. Lett.* **99** 176602
[24] Giovannetti G, Khomyakov P A, Brocks G, Karpan V M, Van Den Brink J and Kelly P J 2008 *Phys. Rev. Lett.* **101** 026803
[25] Bertoni G, Calmels L, Altibelli A and Serin V 2004 *Phys. Rev.* B **71** 075402
[26] Liu S H, Hinnen C, Nguyen Van Huong C, De Tacconi N R and Ho K M 1984 *J. Electroanal. Chem.* **176** 325
[27] Nagashima A, Tejima N and Oshima C 1994 *Phys. Rev.* B **50** 17487
[28] Gierz I, Dil J H, Meier F, Slomski B, Osterwalder J, Henk J, Winkler R, Ast C R and Kern K 2010 arXiv:1004.1573v1
[29] Yamakage A, Imura K-I, Cayssol J and Kuramoto Y 2009 *Europhys. Lett.* **87** 47005
[30] Varykhalov A, Sánchez-Barriga J, Shikin A M, Biswas C, Vescovo E, Rybkin A, Marchenko D and Rader O 2008 *Phys. Rev. Lett.* **101** 157601
[31] Bihlmayer G, Koroteev Y M, Echenique P M, Chulkov E V and Blügel S 2006 *Surf. Sci.* **600** 3888